

Nanofabrication/Nano-Characterization – Calixarene and CNT Control Technology –

ISHIDA Masahiko, FUJITA Junichi, NARIHIRO Mitsuru, ICHIHASHI Toshinari, NIHEY Fumiyuki, OCHIAI Yukinori

Abstract

The world of nanotechnology is plagued by its size limitations and frontiers beyond which fabrication or observation are impossible. Engineering and characterization technologies at the nano-scale are critical technologies for breaking through these limitations and frontiers and for obtaining significant advantages.

NEC has developed and commercialized calixarene, an ultra high-resolution resist technology for electron-ray exposure that enables nanofabrication at the 10nm level, and has applied it in the development of nanodevices. Also developed is the technology for preparing metallic nanoparticles at the 1nm level, which is even smaller than the resolution for calixarene. This technology has been applied in the control of the properties of the carbon nanotube (CNT). NEC has also succeeded in observing the process of CNT growth by combining the 3D nanofabrication technology with that of transmission electron microscopy, which is an excellent nano-characterization technology.

Keywords

carbon nanotube, nanoparticles, electron beam exposure, calixarene, transmission electronic microscopy, focused ion beam

1. Introduction

Bottom-up type technology applying technologies such as self-assembly has led to the successful creation of materials with new properties such as fullerene and the carbon nanotube (CNT). However, since the new materials resulting from this bottom-up technology are difficult to handle due to their very small sizes, it is often very hard to find a practical method for applying them.

On the other hand, semiconductor processing technology is the representative top-down type of nanofabrication technology. It has progressed every year and 65nm node products are mass-produced at present. In parallel, a process for the 45nm node, which corresponds to 1/4 of the 193nm wavelength of the ArF laser for use in optical lithography, is also being developed. Additionally, nanofabrication of sizes below 10nm are also becoming possible by using electron beam lithography, although mass-production methods using this technology is still delayed.

The development of these technologies has brought the level of nanotechnology to a point close to a direct connection of the bottom-up type materials and the top-down type nanofabrication/nano-evaluation technologies (Fig. 1).

This paper introduces the efforts that are being made in the

field of nanotechnology at NEC. These include calixarene resist technology that has made nanofabrication possible at 10nm or less and a new technology (LANS) that applies calixarene to expand the domain of top-down type technology and has made the fabrication of metallic nanoparticles possible at the 1nm level. The application of LANS for enabling the control of CNT properties and the elucidation of its growth mechanism and attempts to directly observe nano-scale phenomena by means of transmission electron microscope (TEM) are also discussed.

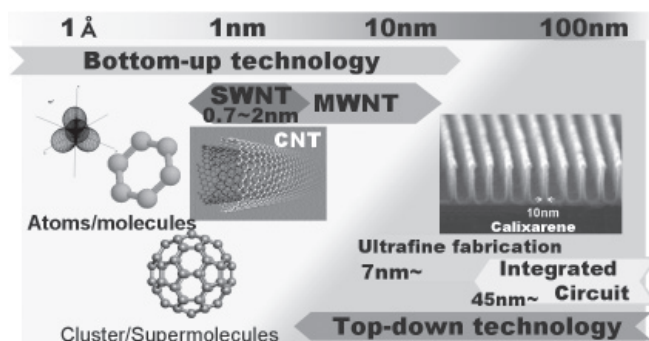


Fig. 1 Positioning of bottom-up and top-down technologies.

2. Development of Calixarene Resist

In general, the resolution of resist is roughly dependent on the molecular weight of the resist material. This means that a finer pattern with less roughness can be fabricated by using a resist with a lower molecular weight. However, since the reduction of molecular weight theoretically drops the sensitivity and the glass transition temperature, materials with low molecular weight tend to have properties that are unsuitable for use with resists, for example, the impossibility of becoming a solid at normal temperatures or an increase in roughness due to the highly crystalline characteristics. As a result, there are few resist materials that have both favorable properties and low molecular weights.

Among these materials, we have been researching into calixarene because it has a stable cyclic structure in spite of its low molecular weight and also features very favorable properties for use as high-resolution resists¹⁾. We have actually attempted its application at the R&D level by fabricating a nano MOS-FET with an 8nm gate length using calixarene resist and predicting the limit size at which the MOS-FET can function²⁾.

Nevertheless, the poor solubility of traditional calixarene resist has forced us to use an organic chloride solvent that is

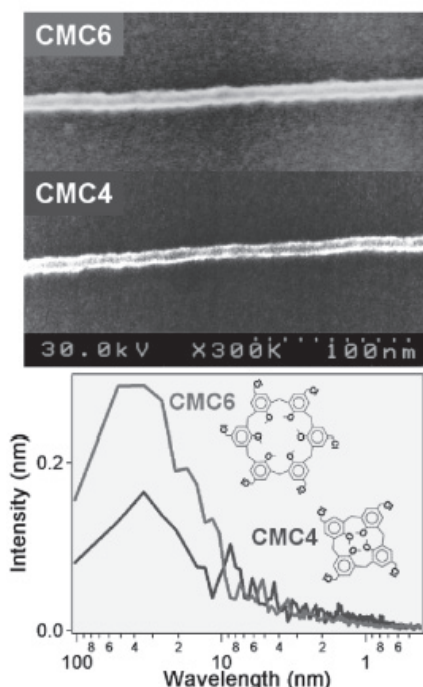


Fig. 2 Comparison of calixarene resists.

known to be harmful, this issue has been regarded as one of the factors hindering its industrial application. To deal with this problem, we conducted joint development together with the Tokuyama Corporation of a calixarene that can be dissolved in a safe solvent. We eventually determined that chloromethyl methoxycalix[4]arene (CMC4), which has the same structure as the traditional chloromethyl methoxycalix[6]arene (CMC6) except that the number of the units forming the ring is reduced by two, presents very favorable properties³⁾.

Fig. 2 shows the result of a comparison of the minimum line widths of the fine resist lines fabricated by using CMC6 and CMC4. The line width of the CMC4 is clearly thinner than that of the CMC6. The minimum line width available with CMC4 was about 7.3nm, which was more than 15% lower than for the previous material. The graph at the bottom of Fig. 2 shows the results of the analyses of the edge roughness of the patterns fabricated with CMC6 and CMC4 by decomposing them into the interval component. The roughness of intervals longer than 10nm is reduced considerably with CMC4. In addition, the solubility is also improved with CMC4, confirming that it is dissolvable to almost any safe solvent.

The reason that such an improvement was obtained by simply reducing the construction units has been clarified by an X-ray diffraction analysis. While CMC6 resist films presented a peak of molecule crystallization that of CMC4 resist did not present such a peak. It was found that, CMC4 is difficult to crystallize and thus can improve the solubility, resolution and roughness because CMC4 has a cyclic structure and can maintain a random structure in spite of its low molecular weight.

At present, CMC4 resist is marketed by Tokuyama Corporation with the product name of TEBN-1. As the organic resist

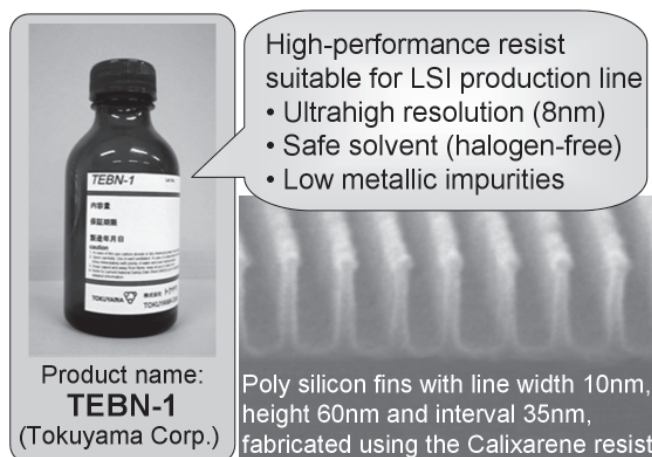


Fig. 3 TEBN-1, calixarene resist product.

with world's highest resolution, it is used widely in the development of most advanced devices or as the benchmark of electron beam lithography systems (Fig. 3).

3. Nanoparticle Patterning at 1nm Level

The development of calixarene resist has advanced the electron beam lithography into the resolution below 10nm, but there are still some gaps remaining before direct handling of bottom-up type materials at the 1nm level such as the carbon nanotube (CNT). Therefore, we tackled the fabrication of metallic nanoparticles by applying the calixarene resist technology.

The bottom-up type technology for fabricating metallic nanoparticles has already made it possible to fabricate 1nm level nanoparticles of uniform size as a result of the development of techniques such as the inverse micelle method. But it has been difficult to apply the fabricated nanoparticles in devices because these techniques mainly need synthesis in solutions.

We therefore developed LANS (Lithographically Anchored Nanoparticles Synthesis), which is a completely new synthesis technique using the solid resist pattern itself as the reaction container in the nanoparticles synthesis. We thus succeeded in fabricating nanoparticles with a one order of magnitude smaller size than the resist resolution in a desired position⁴.

Fig. 4 shows the explanation of the LANS process in (a) to (d), the pattern of the iron nanoparticles fabricated with LANS in the atomic force microscopy (AFM) image, and the plot of

the location errors of the nanoparticles.

The process of nanoparticle fabrication using LANS is as follows: First, an electron-beam resist film in which organic metallic molecules are added is fabricated on the substrate (a). Next, a fine dot pattern is formed by electron beam exposure (b), and then metallic nanoparticles are deposited by heating in a vacuum (c). Finally, the carbon component is eliminated from the resist by means of oxygen plasma processing to obtain a substrate on which only the nanoparticles are left in the positions where the resist pattern existed (d).

The features of LANS lie in the possibility of defining the nanoparticle size according to the amount of organic metal molecules mixed and the size of the resist pattern and that of strictly controlling the nanoparticle positions. The nm-level control of the nanoparticle positions has been impossible with traditional fine particle fabrication methods and made possible for the first time by LANS.

Since the nanoparticles fabricated with LANS have a size that is difficult to observe with scanning electron microscopy, we evaluated them with AFM. The AFM image in Fig. 4 shows the pattern of the iron nanoparticles with an average height of about 4nm. We have confirmed that, with iron, nanoparticles as small as 1.7nm can be fabricated. In this case, however, confirmation of their presence is even difficult with AFM. With regard to the special feature that is the position control property, the plot in Fig. 4 shows that all of the nanoparticles are located in positions within ± 20 nm of the target, and that the deficiency rate was nearly 0%.

The development of LANS means that top-down type technology is now capable of reaching the 1nm level domain, also opening the way to an expansion of applications in the future. One attempt for its application is the CNT characteristic control that we will describe in the next section.

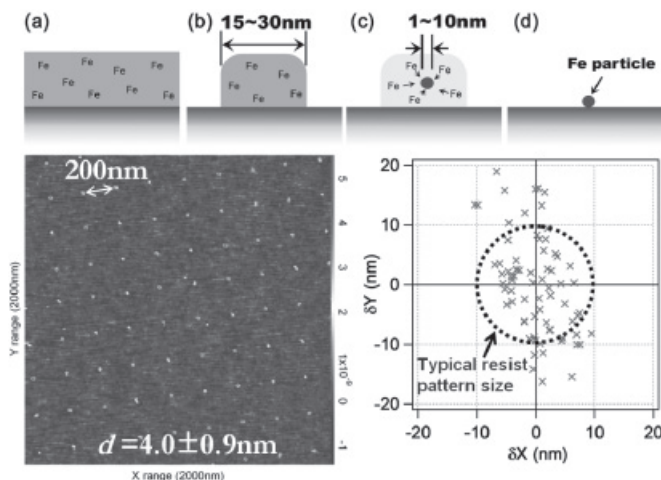


Fig. 4 LANS process flow and characterization of the fabricated fine iron particle

4. Carbon Nanotube Growth Control

The carbon nanotube (CNT) presents the properties of either metal or semiconductor depending on the way the graphite sheet is rolled (chirality). In fact, since it was reported that it is applicable as the material of Field Effect Transistor channels, research has been actively conducted into CNT as a suitable device material. The nanofabrication of Si devices has now almost reached its limit and property degradations due to physical factors such as decreases in the mobility and increases in the leak current have become noticeable. The CNT properties such as its high mobility, high withstanding of current density and the high chemical stability of surfaces thus make CNT a

truly attractive material for spin-on transistors and post-Si semiconductors.

Nevertheless, most of the currently available CNT devices such as the multi-walled nanotube (MWNT) with from two to some tens of graphite sheet walls and the single-wall nanotube (SWNT) with a single graphite sheet wall are available as an assembly containing both metallic and semiconductor elements. As a result, the key to applying them in electronic devices has become how to selectively obtain the semiconductive SWNT element from them.

To deal with this issue, we attempted selective growth of SWNT using iron catalyst nanoparticles fabricated with LANS. Usually, CNT grows by supplying the carbon material to the metallic particles that play the role of catalyst in the vapor phase. Our test used iron nanoparticles with an average diameter of 1.7nm that were patterned at the 100nm pitch. We attempted to grow the SWNT by heating the nanoparticles to 750°C in a vacuum to supply the carbon material that was ethanol.

The AFM image in **Fig. 5** shows the results of observations of the substrate after growth. A large number of thin, linear CNT structures can be observed on the substrate. None of the CNT structures were erected on the substrate but all of them were laid on it, and the lengths were widely distributed from some tens of nanometers to two micrometers at the longest.

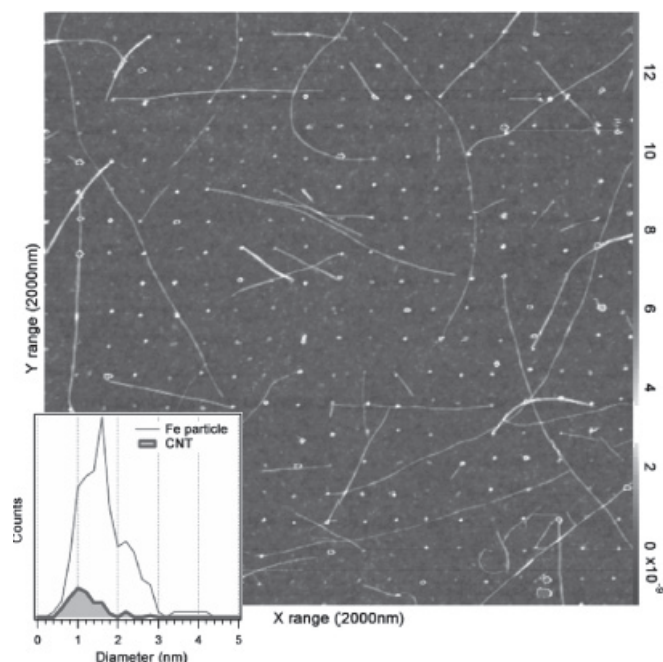


Fig. 5 CNT growth from catalyst prepared with LANS.

The AFM image also shows that almost all of the CNT structures have grown from the grid points of the nanoparticle arrays. As there has been no precedent for growing each and every CNT almost exactly from the point specified by means of lithography, our result can be regarded as a breakthrough.

Also, as shown by the graph in Fig. 5, the diameters of the CNT structures were distributed completely within the size distribution range of the nanoparticles before growth. The CNT diameter distribution after growth was 1.3nm ($1\sigma = 0.4\text{nm}$) while the average nanoparticle diameter was 1.7nm. We also measured the Raman scattering spectrum to confirm the presence of SWNT structures and observed the RBM (Radial Breathing Mode) peaks that are said to be specific to SWNT. The SWNT diameters calculated from the peak positions were 1.22nm and 1.26nm, which corresponded very well to the CNT diameter distribution observed with AFM. The shapes of the peaks also suggested that they are the signals from a single SWNT structure and not bundles. Based on all of the above results, it was highly probable that most of the CNT structures observed in Fig. 5 were SWNT structures, and this made it possible to confirm the effect of the catalyst nanoparticle size control of LANS⁴⁾.

5. In Situ Observation of Carbon Nanotube Growth

Since the growth of CNT occurs around fine metal particles at the nm level size, the difficulty in identifying the detailed mechanisms has also been attracting attention from the viewpoint of nano-characterization.

According to the knowledge accumulated up to the present, in the initial stage of CNT growth, metallic nanoparticles heated to a high temperature absorb hydrocarbon gas from the ethylene or alcohol supplied as the material, and form a eutectic state between metal and carbon. At this time, it is said that the melting point that is usually above 1,200°C drops to around 600°C because of the effects of the nanometric size and eutectic state. When the carbon in the nanoparticles in the eutectic state are oversaturated to a certain degree, the nanoparticles begin to eject the carbon as the CNT structures, beginning the growth state in which supply of the carbon material and ejection of the CNT structures occur successively. The maximum growth rate is as high as 1 $\mu\text{m}/\text{sec}$ or more. This means that CNT structures of more than 1,000 times larger than the nanoparticle catalyst with about 1nm diameter are ejected in a single second.

However, the phenomena described above are merely esti-

mated from the situations and they have never been observed directly. So we attempted to observe the CNT growth directly by combining the 3D nanofabrication technology using focused ion beam (FIB) and electron beam and the nano-characterization technology based on transmission electron microscopy (TEM)⁵.

Firstly, to enable TEM observation that requires a high degree of vacuum, we began the study with the method for supplying the carbon material in the solid state, although it is usually supplied in the gas state. **Fig. 6** shows the beam-induced vapor-phase deposition technology we used to fabricate the amorphous carbon (a-C) nanopillars for use as the template for the CNT growth. With this technology, the material supplied in the gas state and decomposed and deposited locally using a beam focused at the nanometric level in order to fabricate the structures. When carbon hydride gas is used as the material, it is possible to fabricate nanometric a-C 3D structures that are suitable for the CNT growth.

We used this technology to fabricate an a-C base block with doped iron and fine a-C pillars (about 10nm) without doped iron as shown in the model diagram in **Fig. 7**. When the fabricated sample was heated in a vacuum, the iron in the base started agglomeration at about 500°C and particles began to move around at over 600°C. This is the process by which a-C is changed by iron nanoparticles into the more stable graphite carbon (g-C), in which a-C is captured by the iron nanoparticles and ejected as g-C in the same way as the CNT growth. The successive TEM images shown in Figs. 7 (a) to (e) show the results of observations at every 2 seconds in the period when an iron nanoparticle penetrates into an a-C pillar.

These images show the process of the gradual advance of an iron nanoparticle inside a pillar as if they are capturing a-C in it, until a graphite tube with about 10 walls and almost the same diameter as the original pillar is ejected. This can be considered as a completely identical phenomenon to the process

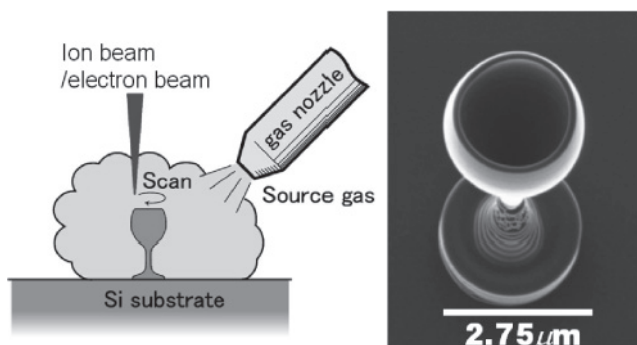


Fig. 6 Beam-excited vapor-phase deposition technology.

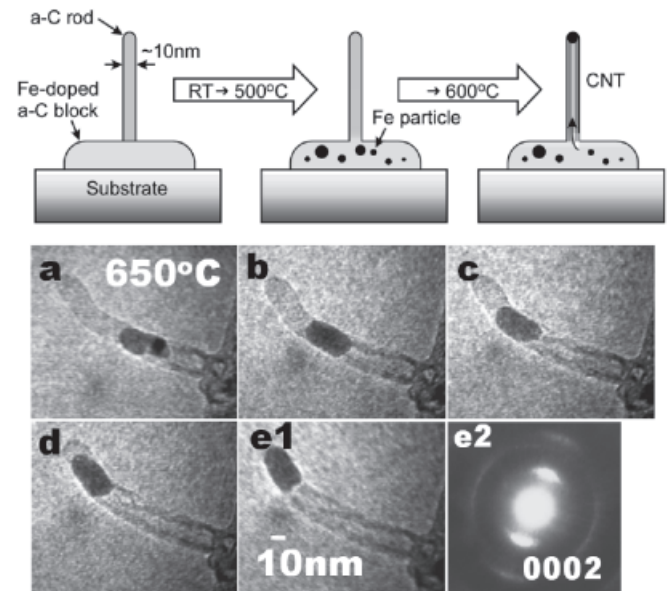


Fig. 7 In situ observation of CNT solid-phase growth.

of CNT growth. In fact, the diffraction pattern obtained from the pillar after reaction (f) allows us to observe the diffraction of graphite from the 0002 plane.

The nanoparticles migrate by changing their shapes like a liquid during a reaction and behavior as if there was surface tension at their surfaces was also observed. At the same time, however, they also presented phenomena suggesting the presence of crystallinity, for example image density variation called “moiré interference fringe” such as that seen on the nanoparticle in (a). This indicates that the nanoparticles during growth have the properties of both liquid and solid at the same time. In addition, other previously unknown facts were also clarified as a result of analyses, such as the fact that the carbon is mainly transported on the surface layers of the iron nanoparticles.

6. Conclusion

As described above, we are conducting basic properties research in materials searches and applications developments using our advanced nanofabrication/nano-evaluation technologies. We propose to lead the knowledge obtained through this research to breakthroughs in existing technologies and proposals for new enterprises.

References

- 1) Fujita, J., Ohnishi, Y., Ochiai, Y., and Matsui, S., Appl. Phys. Lett. 68, 1297 (1996);
Fujita, J., Ohnishi, Y., Manako, S., Ochiai, Y., Nomura, E., Sakamoto, T., and Matsui, S., Jpn. J. Appl. Phys. 36, 7769 (2000).
- 2) Kawaura, H., Sakamoto, T., and Baba, T., Appl. Phys. Lett. 76, 3810 (2000).
- 3) Ishida, M., Fujita, J., Ogura, T., Ochiai, Y., Ohshima, E., and Momoda, J., Jpn. J. Appl. Phys. 42, 3913 (2003).
- 4) Ishida, M., Hongo, H., Nihey, F., and Ochiai, Y., Jpn. J. Appl. Phys. 43, L1356 (2004).
- 5) Ichihashi, T., Fujita, J., Ishida, M., and Ochiai, Y., Phys. Rev. Lett. 92, 215702 (2004).

Authors' Profiles

ISHIDA Masahiko

Assistant Manager,
Nanotechnology Group,
Fundamental and Environmental Research Laboratories,
NEC Corporation

FUJITA Junichi

Assistant Professor,
Graduate School of Pure and Applied Sciences,
University of Tsukuba
Ex-Principal Researcher,
Fundamental and Environmental Research Laboratories,
NEC Corporation

NARIHIRO Mitsuru,

Assistant Manager,
Silicon Devices Technology Group,
System Devices Research Laboratories,
NEC Corporation

ICHIHASHI Toshinari

Principal Researcher,
Energy Devices Technology Group,
Fundamental and Environmental Research Laboratories,
NEC Corporation

NIHEY Fumiyuki

Principal Researcher,
Nanotechnology Group,
Fundamental and Environmental Research Laboratories,
NEC Corporation

OCHIAI Yukinori

Program officer
Special Coordination Funds for Promoting Science and Technology ,
Japan Science and Technology Agency (JST)
Ex-Senior Researcher,
Fundamental and Environmental Research Laboratories,
NEC Corporation